Received: 2 July 2021 | Revised: 8 September 2021 | Accepted: 23 September 2021

DOI: 10.1002/elsc.202100081

Engineering in Life Sciences

REVIEW

3D printing in biotechnology—An insight into miniaturized and microfluidic systems for applications from cell culture to bioanalytics

Christopher Heuer[1] | **John-Alexander Preuß**[1] | **Taieb Habib**[1] | **Anton Enders**[1] | **Janina Bahnemann**[1,2]

[1] Institute of Technical Chemistry, Leibniz University Hannover, Hannover, Germany

[2] Cell Culture Technology, Faculty of Technology, Bielefeld University, Bielefeld, Germany

Correspondence
Janina Bahnemann, Institute of Technical Chemistry, Leibniz University Hannover, Hannover, Germany.
Email: jbahnemann@iftc.uni-hannover.de

Abstract

Since its invention in the 1980s, 3D printing has evolved into a versatile technique for the additive manufacturing of diverse objects and tools, using various materials. The relative flexibility, straightforwardness, and ability to enable rapid prototyping are tremendous advantages offered by this technique compared to conventional methods for miniaturized and microfluidic systems fabrication (such as soft lithography). The development of 3D printers exhibiting high printer resolution has enabled the fabrication of accurate miniaturized and microfluidic systems—which have, in turn, substantially reduced both device sizes and required sample volumes. Moreover, the continuing development of translucent, heat resistant, and biocompatible materials will make 3D printing more and more useful for applications in biotechnology in the coming years. Today, a wide variety of 3D-printed objects in biotechnology—ranging from miniaturized cultivation chambers to microfluidic lab-on-a-chip devices for diagnostics—are already being deployed in labs across the world. This review explains the 3D printing technologies that are currently used to fabricate such miniaturized microfluidic devices, and also seeks to offer some insight into recent developments demonstrating the use of these tools for biotechnological applications such as cell culture, separation techniques, and biosensors.

KEYWORDS

3D printing, biosensors, cell culture, microfluidics, miniaturization

Abbreviations: CAD, computer-aided design; DLP, digital light processing; FDM, fused deposition modeling; MJP, MultiJet printing; OD, optical density; PDMS, polydimethylsiloxane; PSi, porous silicon; *S. cerevisiae*, *Saccharomyces cerevisiae*; SLA, stereolithography; SPE, screen printed electrode

1 | INTRODUCTION

In recent years, additive manufacturing techniques—also known collectively as 3D printing—have become widely recognized as a very promising technology, with the potential to revolutionize the biotechnology field. 3D printing was initially developed by Charles (Chuck) W. Hull in 1984, and it was subsequently patented in 1986 as a system that could produce three-dimensional objects in an additive manner, layer by layer [1–3]. Since that time, this young technology has already experienced several major breakthroughs: First, the term 3D printing now describes a variety of different manufacturing methods, the most commonly known and widely used being stereolithography (SLA) [1]; fused deposition modeling (FDM) [4]; selective laser sintering (SLS) [5]; and various inkjet-based techniques, including MultiJet printing (MJP) [6]. Each of these methods has its own specific relative advantages and disadvantages—resulting in specific areas of preferred applications for all of them. SLA, for example, enables the production of the finest structures compared to the other technologies [7, 8]. By contrast, FDM printers offer significantly higher accessibility due to their relatively low acquisition cost [9]. In addition, FDM printers can use a wide range of biocompatible thermoplastic polymers, which further expands their potential range of applications [10–12].

Second, the operation of modern 3D printers has become very straightforward, and no longer requires any substantial expertise or training: simply put, computer-aided design (CAD) software is used to create a 3D design, which can then be transferred directly to the printer for manufacturing. The ability to create complex 3D structures in a simple and flexible fashion sets this technology apart from more conventional methods for constructing miniaturized and microfluidic systems fabrication—such as soft lithography with polydimethylsiloxane (PDMS), which requires a unique master mold for each design [13].

Third, key features (such as printing resolution and speed) have also significantly improved over the years. For instance, while the first commercially available 3D printer (SLA-1) took an entire day to print even simple prototypes [3], modern 3D printers can print structures with dimensions of as low as 20–30 μm within just a few hours [14]. Collectively, these technological advancements in the field of 3D printing now enable advanced modern 3D printer systems to create rapid prototyping systems through which researchers can test varying experimental parameters before fabricating miniaturized microfluidic systems. Furthermore, concurrent advances in material sciences have led to the development of a wide and ever-growing array of printing materials with various useful properties, such as translucence, heat resistance, and biocompatibility [15–17]—making this technology more and more attractive for researchers working within the biotechnology field.

This review aims to explain additive manufacturing techniques relevant to biotechnology applications, and give an insight into some of the many opportunities that modern 3D printing techniques have to offer. We focus on miniaturized and microfluidic 3D-printed devices made from plastic polymers for utilization in microbial and mammalian cell culture and bioanalytics (e.g. chromatography, electrophoresis, biosensors, etc.) and highlight relevant examples mainly drawn from the last 5 years.

2 | 3D PRINTING TECHNIQUES

The fundamental insight underlying the concept of 3D printing is to imagine that all three-dimensional objects are the total sum of their various 2D elements—which can be built up upon each other, layer by layer. Accordingly, if a CAD model of the desired object is sliced into a finite number of 2D layers (dependent on the resolution of the 3D printer), those layers can then be used to inform a 3D printer how to assemble the entire object, layer by layer [18, 19]. A popular file format to be loaded in the slicing software is Standard Tessellation Language (.STL), which describes an object's surface geometry as a number of triangles [87].

In the literature, several 3D printing techniques (all with different comparative advantages and disadvantages) have been described for the manufacturing of microfluidic and miniaturized devices using various materials. SLA was the first established and patented technique: in this approach, a liquid photopolymer is precisely cured at a designated location using a laser (see Figure 1A) [20]. A stage or carrier plate is immersed in a bath containing this photopolymer and a photoinitiator, and its Z position can be moved stepwise to define the printing height of each layer. Since a laser must cure every spot, the printer's resolution is limited by the minimum pixel size of the laser beam [20]. SLA offers both the best resolution and lowest surface roughness of all the 3D printing techniques surveyed in this chapter. Channel dimensions below 30 μm have been reported in the literature [21]. A further refinement aimed at improving the low printing throughput of SLA was the development of digital light processing (DLP), which offers the ability to cure all relevant spots of a layer in parallel [22]. SLA and DLP do not require additional support materials, but the photopolymer solution needs to be removed after the printing procedure. In addition to commercialized materials, various self-defined formulations of biocompatible and transparent materials such as polyethylene glycol diacrylate can also be employed as printing materials using these techniques [21, 23]. However, it should be

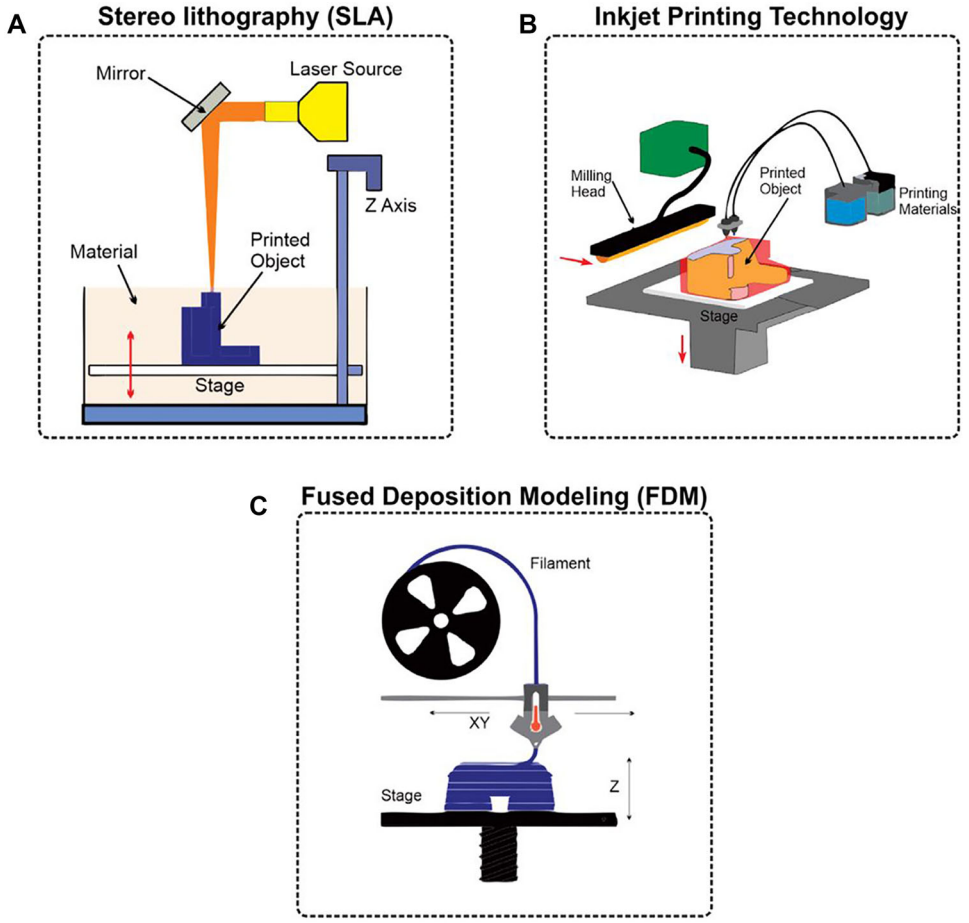

FIGURE 1 Principles of 3D printing techniques. (A) In stereolithography (SLA) a movable stage is immersed in a bath containing a photopolymer and a photoinitiator. A laser is used to cure the polymer material at designated positions. (B) During inkjet-based printing, main and support materials are dropwise applied onto a stage, and the main material is cured using UV light. A milling head or leveling blade is used to smooth the surface after a layer is finished. (C) Fused deposition modeling (FDM) uses filaments of thermoplastic polymers that are heated and subsequently applied layer by layer to create the 3D object. Adapted with permission from [45]. Copyright 2018, the authors. Published under Creative Commons Attribution 4.0 International license (CC BY 4.0)

noted that residual non-reacted photoinitiators can impair biocompatibility, and that the light absorptive properties of the photopolymer might affect the printing resolution [20].

Inkjet-based techniques such as MJP and PolyJet printing (these actually constitute the same technology issued by different manufacturers) are a popular alternative since they utilize a high degree of automation and also result in a high-quality end product [20]. In this technology, main and support material are applied dropwise through printheads consisting of an array of nozzles (see Figure 1B). The main material is usually a proprietary acrylate, which is then cured using UV light [22, 24, 25], while the support material enables the fabrication of overhanging and complex 3D structures by filling cavities and hollows such as microfluidic channels—although this support material must ultimately be removed after the printing procedure is completed [25, 26]. Different commercial suppliers offer numerous materials with different properties (e.g. rigid, flexible, transparent, biocompatible, high-temperature resistant [15, 27, 28]. Unfortunately, the exact formulation of these commercialized materials is often not publicly available, and, as a result, the bioactivity of any such material must first be investigated carefully prior to use, as some of these materials may release potentially non-biocompatible leachables [20]. In addition, since all materials are applied dropwise, the overall resolution depends on the droplet size [22]—although this still permits the fabrication of channel dimensions in the range of hundreds of micrometers and below [29–32].

Last but not least, FDM is the cheapest technique for 3D printing of miniaturized devices. This technology belongs to the extrusion-based methods, as a printhead heats thermoplastic filaments above the melting point and then applies them onto a surface to let them cool (see Figure 1C) [20]. Instead of an external support material being used to filling cavities, fragile support structures are themselves

printed—which facilitates the creation of overhanging structures. The main advantages of FDM are the free choice of material (e.g. acrylonitrile butadiene styrene (ABS) [33], polyethylene terephthalate glycol (PETG) [18], polylactide acid (PLA) [18, 34, 35], polyurethane [36], etc.), the ability to use multiple materials within a single 3D-printed object, and the option to intervene in the printing process [18, 37, 38]. The main disadvantages posed by this technique are the usage of heat-sensitive materials (thermoplastics), the risk of potential fluid leakage due to an incomplete infill of the filamentous structures, and the difficulty of printing integrated channels [39]. This method also has the highest roughness and the lowest printing resolution out of all of the techniques surveyed in this paper [22, 40]. Nonetheless, even using FDM, channel dimensions down to 40 μm have still been reported [36]—although channel dimensions in the range of hundreds of micrometers are far more common [34, 35, 41].

It should be emphasized that the 3D printing technology and material have to be selected carefully and with the specific goals of a given project in mind, since there is no universal material that is best suited (or even appropriate) for all conceivable applications. For usage in biotechnology, desired material properties that must be carefully considered include biocompatibility, gas permeability, and the option to be sterilized. In FDM, commonly used materials such as ABS and PLA are biocompatible—but the fabrication of transparent devices and integrated microfluidic channels can be challenging [13, 42]. Some materials, such as the commonly used PLA, are heat-sensitive and thus not suited for heat steam sterilization; however, heat-resistant alternatives for FDM exist. Photocurable materials such as polyacrylates (typically used in SLA and inkjet-based techniques) are better suited to create transparent devices, the development of integrated microfluidic channels is more straightforward, and heat steam sterilizable materials are also available [13, 27, 42]. However, researchers should bear in mind that photopolymers may have cytotoxic properties, and comprehensive biocompatibility studies for many commercially available materials are often nonexistent [13, 20]. Nevertheless, there are also examples of such biocompatible resins used in SLA and inkjet-based techniques [15, 43].

It is also dangerous to attempt to generalize about the biocompatibility of any 3D printing material. For example, Rimington et al. have demonstrated that the same 3D printing material had varied cell-specific effects in terms of proliferation and differentiation for different cell types [44]; Siller et al. have demonstrated that even post-processing can have a significant effect on the biocompatibility [15]. This underscores, once again, that the material used for any given project must be selected, taking into account both the cell type(s) and the application(s) in question.

In terms of gas permeability, however, it can generally be stated that 3D-printed plastic materials used in SLA, inkjet-based techniques, and FDM tend to have relatively poor gas permeability [13]. For further reading, we would refer the reader to the excellent review article of Bhattacharjee et al. who give a detailed overview of various properties of plastic materials used in SLA, FDM, and inkjet-based 3D printing technologies [13].

3 | 3D-PRINTED DEVICES FOR MICROBIAL AND CELL CULTURE

Due to the wide availability of biocompatible materials, 3D printing allows for the fabrication of microbioreactors, cultivation vessels, and other devices for microbial and mammalian cell culture applications. Various studies have now demonstrated the biocompatibility of diverse materials that are compatible with different 3D printing techniques [15, 43, 46]. For instance, Siller et al. have comprehensively studied the biocompatibility of polyacrylate materials used in inkjet-based 3D printers for the cultivation of mesenchymal stem cells (MSCs) according to EN ISO 10993-12 (2012). The viability of cells was measured by various assays (Cell Titer Blue assay, lactate dehydrogenase assay, flow cytometry, real-time live-cell imaging) and found to be unaffected by the polyacrylate materials themselves [15, 47]. However, post-processing and sterilization/disinfection procedures were found to exert significant effects on cell growth and viability [15].

3.1 | Microbioreactors for microbial cultivation

Miniaturization is one of the most significant advantages offered by microbioreactors during bioprocess optimization. These systems significantly reduce the required volumes of cell culture media—thereby enabling researchers to run several experiments at varying conditions in parallel, while also conducting them in a highly space-efficient manner. Furthermore, 3D printing facilitates rapid prototyping of microbioreactors at a comparatively low price, since adapting the CAD file permits simple reactor design adjustments. One example of such a miniaturized system was presented by Panjan et al. who developed a microbioreactor (1 mL internal volume) fabricated by SLA procedure to cultivate *Saccharomyces cerevisiae* (*S. cerevisiae*) with integrated optical density (OD) and real-time glucose monitoring [48]. Figure 2A-i depicts the reactor design consisting of its main cultivation chamber, including a connection port for glucose biosensor integration, an inlet and outlet for liquids, and a gas outlet on top

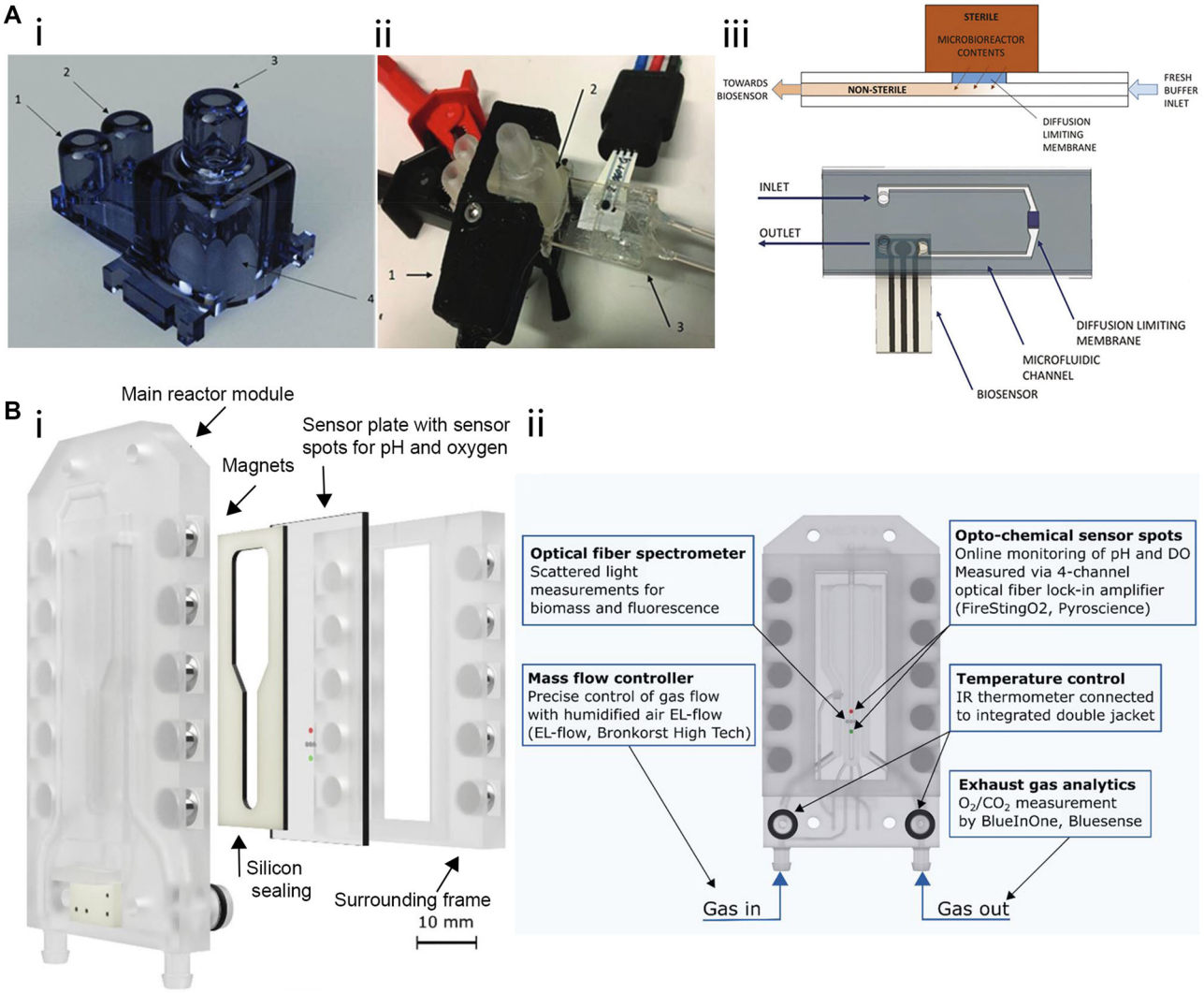

FIGURE 2 3D-printed microbioreactors for microbial cultivation. (A-i) 3D-printed microbioreactor consisting of (1) inlet (2) outlet (3) gas outlet and (4) the main reactor chamber with biosensor integration port. (A-ii) In the experimental setup, a (1) OD sensor is clipped onto the (2) reactor chamber, and the (3) glucose biosensor is integrated. (A-iii) Sterile integration of the glucose biosensors guaranteed by separating the microbioreactor and the biosensing unit with a diffusion limiting membrane. Adapted with permission from [48]. Copyright 2018, the Royal Society of Chemistry. Published under Creative Commons Attribution-NonCommercial 3.0 Unported license (CC BY-NC 3.0). (B-i) Exploded view of the micro bubble column reactor consisting of the main reactor module, sensor plate within a surrounding frame, and silicon sealing being held together by magnets. (B-ii) Schematic of the reactor depicting the position of microsensor spots for process analysis, gassing in-, and outlet as well as the connectors for temperature control. Adapted with permission from [49]. Copyright 2021, the authors. Published under Creative Commons Attribution 4.0 International license (CC BY 4.0)

of the reactor. Placing two small polytetrafluoroethylene (PTFE)-covered magnetic balls inside the microbioreactor enabled magnetically mediated mixing during the cultivation process. Figure 2A-ii depicts the experimental setup, which included a clipped-on OD sensor and an integrated electrochemical glucose oxidase biosensor. Integration of such biosensors for process control in microbioreactors is particularly challenging since the sterility of the system needs to be guaranteed. In the presented work, this challenge was overcome by connecting the reactor chamber to a microfluidic channel via a diffusion limiting membrane (see Figure 2A-iii). This membrane prevented contamination, while still allowing glucose slowly to pass through (i.e. from the reactor to the non-sterile microfluidic channel) and be flushed towards the biosensor. As a proof-of-concept, this microbioreactor system successfully monitored *S. cerevisiae* growth and glucose consumption in real-time over a cultivation period of 8 h.

In another article, Frey et al. reported the development of a customized 3D-printed micro bubble column reactor system (fabricated by MultiJet printing) and demonstrated its successful integration with various microsensors for

bioprocess control during the cultivation of *S. cerevisiae* [49]. In this system, gassing occurred from the reactor bottom, causing air bubbles to rise through the reactor chamber. Fluids (e.g. culture medium) in the microbioreactor were thereby agitated, preventing concentration and temperature gradients without using stirrers. Figure 2B-i depicts an exploded view of the microbioreactor components: The main reactor module sets the shape of the device and provides channels for temperature and gas transfer control. The sensor plate containing microsensing elements, a surrounding frame, and silicon sealing creates the reactor volume by being tied to the main reactor module with magnets. Furthermore, the overall system is clamped together, using a connector clip and screws, in order to avoid leakage. The sensor provides a rapid heat and mass transfer due to the small reactor volume (550 μL), online monitoring of process parameters (biomass, dissolved oxygen, pH), and exhaust gas analysis (O_2, CO_2). Figure 2B-ii depicts a schematic of the reactor detailing the position of microsensor spots for process analysis, gassing in, and outlet, as well as the connectors for temperature control. During an *S. cerevisiae* cultivation over a 16 h period, the process parameters were successfully monitored. In terms of the growth rate, the 3D-printed micro bubble column reactor achieved similar values (0.403 $\pm$ 0.02 h^{-1} at 20 g L^{-1} glucose) compared to conventional systems such as a 2.5 L stirred-tank bioreactor in batch mode (0.4 h^{-1} at 30 g L^{-1} glucose) [50].

3.2 | Applications in mammalian cell culture

Microbioreactors also hold great promise for application in the field of mammalian cell culture; for example, Quian et al. have recently fabricated miniaturized 3D-printed spinning bioreactors to generate and culture forebrain-specific organoids derived from human-induced pluripotent stem cells [51]. These organoids are small organ-like cell structures that can be artificially produced from embryonic, adult, and induced pluripotent stem cells, and as such they are highly useful for disease modeling and drug testing since they resemble "real" organs much more closely than conventional monolayer cultures [51, 52]. Their microbioreactors were created by fitting a 3D-printed cover consisting of 12 spinning shafts and interconnecting gears (created by FDM) onto a standard 12-well plate (see Figure 3A). The gears were driven by a single electric motor, allowing the researchers to sustain organoids in suspension under gentle spinning conditions and thereby preventing aggregation and increasing cell viability compared to static cultures. Miniaturization of the system enables studying organoid generation and performing drug screening and disease modeling under different conditions at lower volumes—which reduces the cost of running experiments compared to deploying larger spinning flasks. As a proof-of-concept application, the forebrain-organoid platform was employed for disease modeling of Zika virus exposure.

Other works have also demonstrated (for example) the usefulness of microfluidic on-chip platforms as blood-brain barrier models [53], microbioreactors for tissue engineering [54], and cultivation chambers for studying angiogenesis (formation of new blood vessels) [55]. These examples underscore the tremendous applicability of 3D printing across a wide variety of cultivation devices and applications.

Aside from the employment of 3D printing technology to fabricate microbioreactors or cultivation devices, additive manufacturing techniques have also been utilized to manufacture other mammalian cell culture-related 3D-printed tools. For example, Alessandri et al. have developed a microfluidic co-extrusion device that enables the production of hydrogel microcapsules to cultivate and differentiate human neuronal stem cells [56]. Production of these hydrogel microcapsules could potentially be used to create a 3D culture system for high-throughput screening, since a massive amount of these stem cell-containing microcapsules can be produced automatically at once. This 3D-printed tool was created by a DLP printer and consists of three inlets (Figure 3B-i) which separately guided fluids into three individual conical layers (Figure 3B-ii), where the outer layers surrounded the inner ones. Three syringe pumps then introduced an alginate solution into the outer layer, an intermediate buffer solution into the middle layer, and the cell suspension supplemented with matrigel (to support stem cell growth) into the inner layer. At the nozzle of the 3D-printed devices, the fluids conjoined and formed droplets with cells encapsulated in them, which were then collected into a calcium gelatination bath (see Figure 3B-iii for the 3-way co-extrusion procedure and production of the hydrogel microcapsules). Neuronal stem cell differentiation into neurons was successfully achieved by culturing the encapsulated cells in a mitogen-free differentiation medium for 13 days; viability was found to be high (~98%), as revealed by 4',6-diamidino-2-phenylindole (DAPI) immunofluorescence.

In a recent project reported by Lavrentieva et al. a 3D-printed device made from polyacrylate material using MultiJet technology was employed to create stiffness gradient hydrogels. These hydrogels are capturing increasing interest in the field of mechanobiology for studying the influence of mechanical cell-matrix (e.g. extracellular matrix) interactions [57]. Reproducible fabrication of these stiffness gradient hydrogels helps researchers to experimentally identify the optimal mechanical conditions for 3D cell

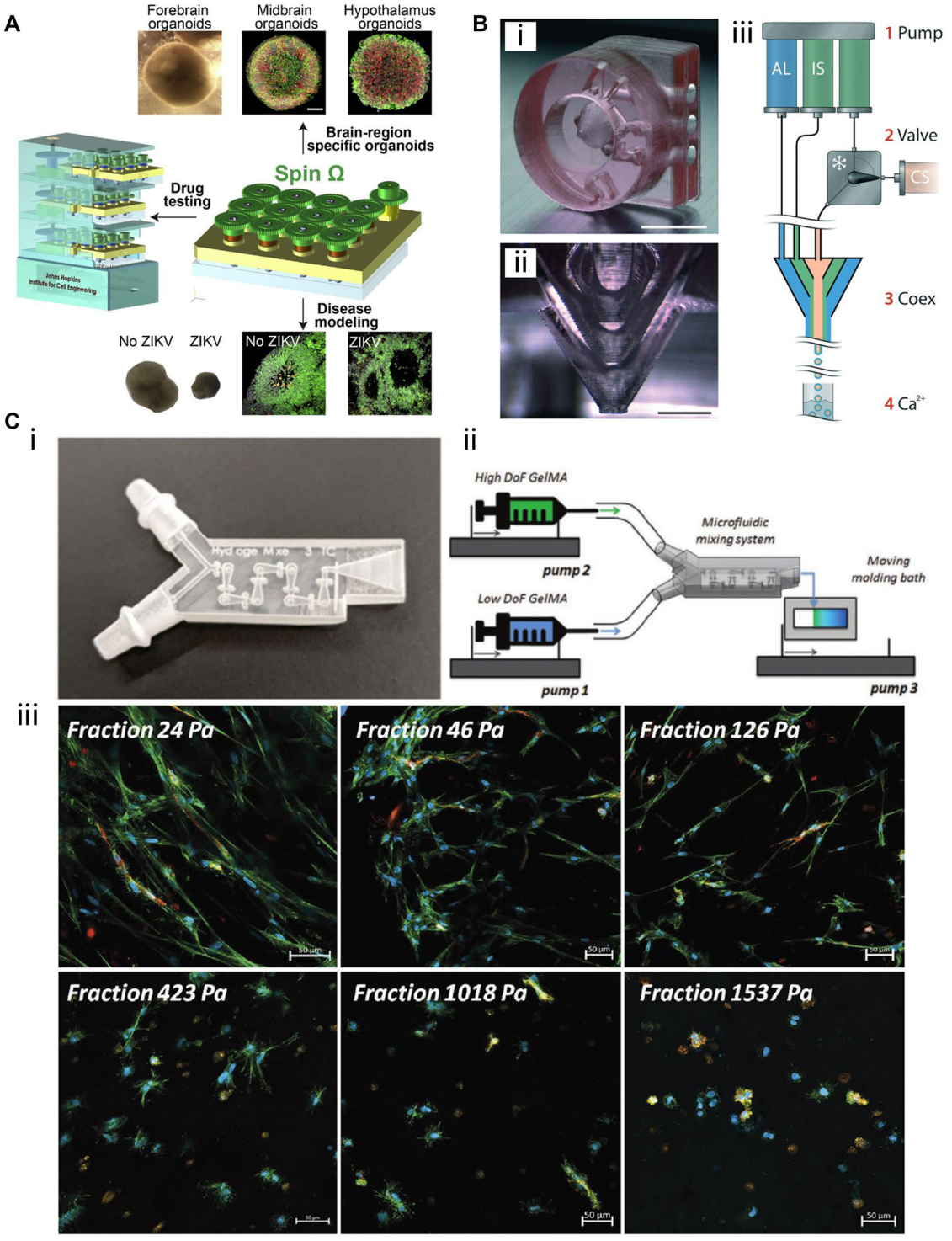

FIGURE 3 3D-printed devices for mammalian cell culture applications. (A) Microbioreactors for forebrain-specific organoid generation and zika virus disease modeling. Reproduced with permission from [51]. Copyright 2016, Elsevier. (B-i) A 3D-printed co-extrusion device with three inlets and (B-ii) three separate conical layers conjoining to form a nozzle is employed to (B-iii) encapsulate human neuronal stem cells into hydrogel microcapsules for high-throughput differentiation. Adapted with permission from [56]. Copyright 2016, the Royal Society of Chemistry. (C-i) A 3D-printed microfluidic mixing device is used to (C-ii) create stiffness gradient hydrogels and (C-iii) study their mechanical influence on cell spreading using various fluorescence dyes for staining. Adapted with permission from [57]. Copyright 2020, the authors. Published under Creative Commons Attribution 4.0 International license (CC BY 4.0)

culture with respect to changes in morphology and cell spreading. In the presented approach, two syringes were connected to the 3D-printed tool, and the gradient was created by pumping hydrogels with high and low crosslinker amounts at varying flow rates into the device. An integrated HC-mixer (as previously described [25]) facilitated homogenous mixing before hydrogels were cast onto a moving molding bath (see Figure 3C-i for a micrograph of the 3D-printed device and Figure 3C-ii for the hydrogel fabrication procedure). Human adipose tissue-derived mesenchymal stem cells (hAD-MSCs) and human umbilical cord vein endothelial cells (HUVECs) cells were then encapsulated into the hydrogel and cultivated for 7 days. These cells were subsequently visualized via staining and fluorescence microscopy (see Figure 3C-iii), and the results demonstrated that cell spreading was increasingly hindered along the gradient with higher stiffness.

3D printing has also been employed to create spiral-shaped inertial focusing devices with potential use for cell culture applications [58]. Such tools are traditionally fabricated via soft lithography (PDMS) or micromilling procedures [58, 59] and were, for instance, demonstrated to isolate T and B cells from blood [60] or isolate single stem cells from stem cell clusters [61]. Such tools have also been used for cell retention integrated into miniature auto-perfusion bioreactors, and as such they can greatly contribute to bioprocess applications [62].

Here, once again, 3D printing offers an alternative to conventional methods that require cleanroom procedures (photolithography/ soft lithography) or are subtractive approaches (micromilling) [58]. Figure 4A depicts an example of a 3D-printed inertial focusing device that can be used to separate bacteria cells using antibody-modified magnetic nanoparticle clusters. In this system, single bacteria are focused near the outer wall of the channel, while larger clusters of bacteria attached to the magnetic nanoparticles are focused towards the inner channel wall (see Figure 4B) and transferred to their respective outlets [63]. The presented device potentially enables the separation of specific bacterial species by choosing the appropriate antibodies.

While 3D-printed inertial focusing devices for bioprocess applications are still rare, we believe that these tools will increasingly be employed for such operations in the future. For example, Enders et al. have shown that these 3D-printed spiral cell separator devices can be used for cell retention to enable continuous cultivation processes [64]. Such systems could also potentially be used to concentrate cells with the aim to improve the transient transfection of mammalian cell lines used for protein production.

We note in passing that 3D printing has mainly been employed for tissue engineering applications by printing scaffolds from various materials and bioprinting (printing of biomaterials and living cells). Because this review aims to explain the application of 3D-printed miniaturized and microfluidic devices made from plastic materials, we do not dwell on 3D printing for tissue engineering; nevertheless, we would refer any interested readers to the review articles of Tamay et al. [65] and Zaszczynska et al.[66].

4 | 3D-PRINTED DEVICES FOR BIOANALYTICS

Bioanalytical methods such as chromatography and electrophoresis are routinely used in biotechnology laboratories to separate and detect nucleic acids and proteins. Biosensors are widely applied to detect various target molecules using appropriate biosensing schemes (e.g. optical, electrochemical, mechanical, etc.) and concepts. Once again, 3D printing offers substantial benefits across all of these applications—including system miniaturization that reduces fluid consumption, and required space and results in lowered experimental cost and greater parallelization opportunities. Moreover, 3D printing also enables rapid prototyping of different experimental setups in a flexible and customized fashion. For example, in terms of biosensor integration into 3D-printed microfluidic systems, parameters such as channel dimensions and geometries, and device size can all be quickly adjusted to fit shifting experimental requirements.

4.1 | Chromatography and electrophoresis

One advantage of 3D printing for chromatography applications is the ability to miniaturize systems, which can be used to combine numerous columns within a single 3D-printed device or miniaturize very long chromatographic columns within one microfluidic lab-on-a-chip tool [67, 68]. One example of such a miniaturized chromatographic system was given by Lucklum et al. who developed stacked spiral miniature 3D gas chromatography columns for potential use in a portable ethylene sensor system during fruits transport and storage [69].

Moreover, the ability of 3D printing to manufacture complex 3D structures enables the production of customized and tailored column beds. While conventional beds are often made out of porous materials with inhomogeneous structures, they can be directly manufactured via 3D printing in an ordered fashion with specific geometries to improve the separation performance [67, 70]. Simon and Dimartino were one of the first to manufacture an ion-exchange adsorber with a DLP printer in a single step, using a customized printing material [71, 72], thereby

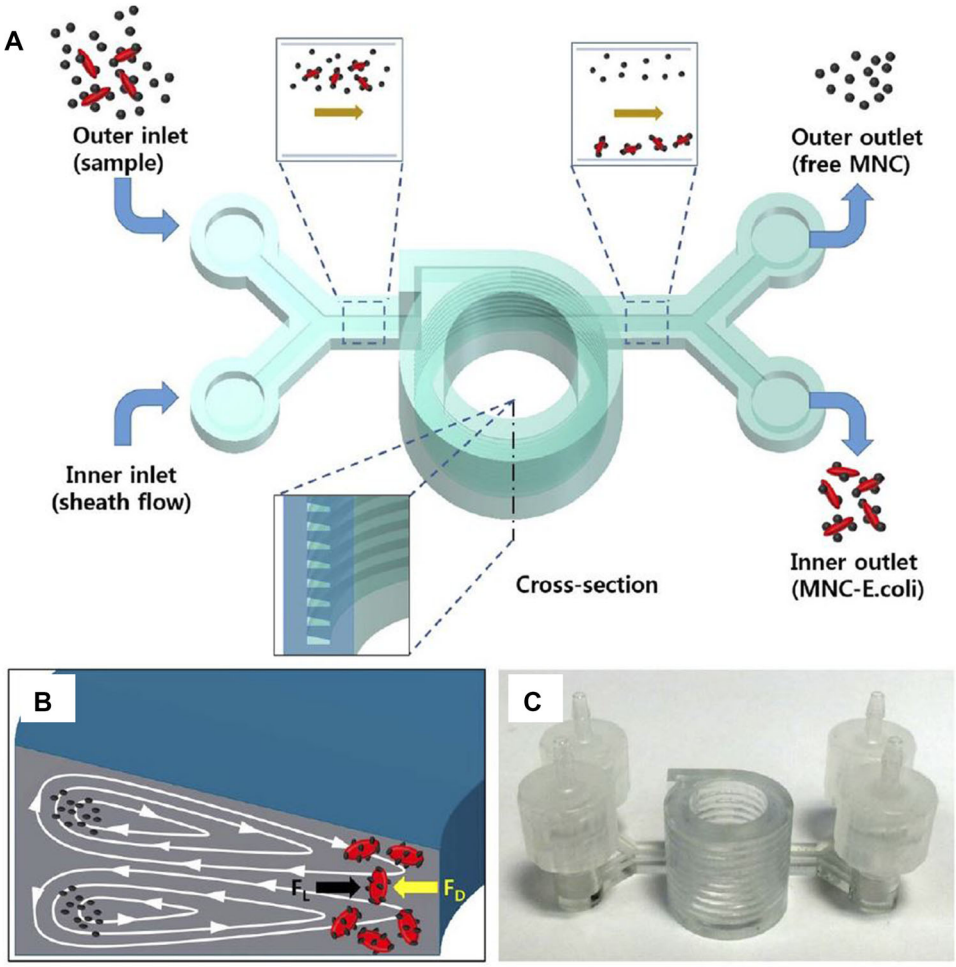

FIGURE 4 3D-printed microfluidic inertial focusing device for bacteria separation (A) Schematic of the 3D-printed spiral-shaped inertial focusing device. Bacteria and antibody-modified magnetic nanoparticle clusters (MNC) are introduced into the system. (B) Single bacteria are focused near the outer wall of the channel, while bacteria attached to the antibody-modified magnetic nanoparticles are focused close to the inner channel wall, enabling separation into designated outlets. (C) Photograph of the 3D-printed tool. Reproduced with permission from [63]. Copyright 2015, the authors. Published under a Creative Commons Attribution-NonCommercial-NoDerivs 4.0 International License

enabling the fabrication of columns with such ordered bed morphology (see Figure 5A). This system was used to separate BSA and myoglobin and purify C-phycocyanin, a bacterial pigment-protein with potential uses in medicine and biotechnology by means of anion exchange chromatography [72].

Although the feature size of the adsorbers bed channels was reportedly larger than in commercial resins (200 μm compared to 50 μm), the separation performance was similar. The authors claim that the improvement of 3D printing resolution within the next few years will likely continue to enhance the comparative performance of these 3D-printed bed columns in comparison to more conventional packaging [72].

With respect to the bed structure design, the ability of 3D printing for rapid prototyping also offers tremendous benefits. For example, different bed structures with various sizes or geometries can potentially be created and expeditiously tested for their separation performances. Figure 5B shows a collection of ordered beds with different geometries (such as spheres, tetrahedra, and triangular bipyramids) that are designed, printed, and characterized in various configurations according to their shape, position, orientation, and plate height. Experimental validations of computations predictions regarding such permutations can be achieved through rapid prototyping of these structures via 3D printing [73].

For the future, we envision integrated and continuous chromatographic units in biotechnological applications. For instance, culture broth from a bioprocess could continuously be forwarded through a chromatographic separation unit for preparative or analytic purposes. The role of 3D printing would be to help achieve the simplification of interfacing across all units. A single 3D-printed microfluidic chip could potentially supersede complex tubing connections, integrate valves for pseudo-continuous

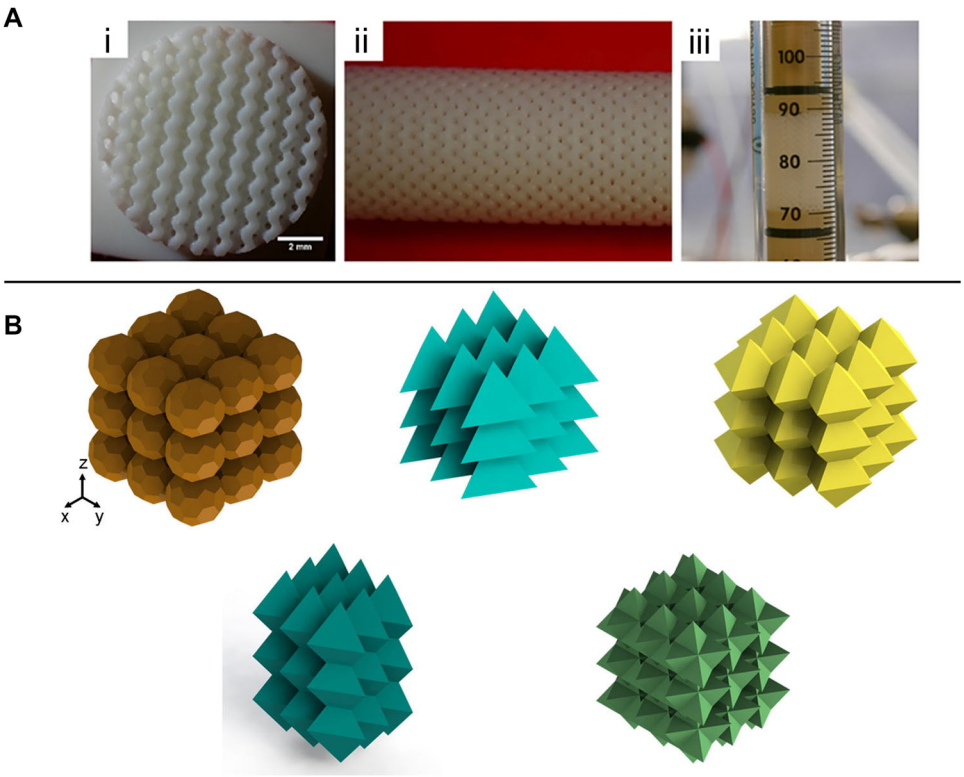

FIGURE 5 (A) 3D-printed anion exchange column with (i-ii) an ordered bed morphology. These ordered cylindrical structures are termed Schoen gyroid structures. (iii) Integration of the 3D-printed structure in a glass column. Adapted with permission from [72]. Copyright 2020, the authors. Published under Creative Commons Attribution 4.0 International license (CC BY 4.0). (B) Bed geometries designed and printed via 3D printing. These structures were experimentally investigated regarding their plate height to confirm computational predictions. Adapted with permission from [73]. Copyright 2017, Elsevier

sample injection. Using customized 3D-printed threads, this interface could integrate any commercialized or self-designed (3D-printed) columns or follow-up analytics (e.g. mass spectrometry) into a single miniaturized and tightly arranged platform. One particularly tantalizing example of how 3D printing can facilitate the integration of high-performance liquid chromatography (HPLC) into a customized and more complex setting was given by Wang et al. in 2017. An end front sample preparation application was developed, which included both microflow injection (μFI) and peak focusing. For the μFI, a 3D-printed multiway valve controlled the access of sample, eluent, and washing buffer towards HPLC, 3D-printed microsolid phase extraction (3D-μSPE) unit, and waste. The 3D-μSPE accomplished peak focusing using polyaniline-decorated magnetic nanoparticles and antimicrobial substances have been detected with a 16-25 fold increase of efficiency in saliva and urine samples [74].

An example of a 3D-printed gel electrophoretic chip (created by MultiJet technology) that proved useful for DNA separation was recently given by Adamski et al. in their work. Figure 6A-i depicts a schematic of this device, which consists of two crossed microfluidic channels where the shorter channel is used to introduce the DNA sample (fluorescently labeled 50 to 800 bp DNA ladder fragments) and transfer it to the longer separation channel, which is filled with electrophoresis gel [75]. The introduced fluorescently labeled DNA fragments (Figure 6A-ii) are then driven through the channel by applying a voltage and separated (Figure 6A-iii and iv). Fluorescence is used to detect the labeled and separated DNA fragment at a designated spot (Figure 6A-v and vi). According to the authors of that publication, this device is the first 3D-printed tool ever reported as being successfully used for gel electrophoretic DNA separation. Notably, this device can also be rapidly fabricated (3 h printing) at a relatively low cost (<1€).

3D printing has additionally been employed to create free-flow electrophoresis systems [33, 76, 77]. This electrophoretic technique separates the analytes in a liquid phase continuously, and does not require a gel-like matrix of the sort utilized in agarose gel electrophoresis and sodium dodecyl sulfate-polyacrylamide gel electrophoresis (SDS-PAGE) for DNA and protein separation, respectively [78]. For example, Preuss et al. have developed a 3D-printed free-flow electrophoresis device with a simple design that can be fabricated from a polyacrylate

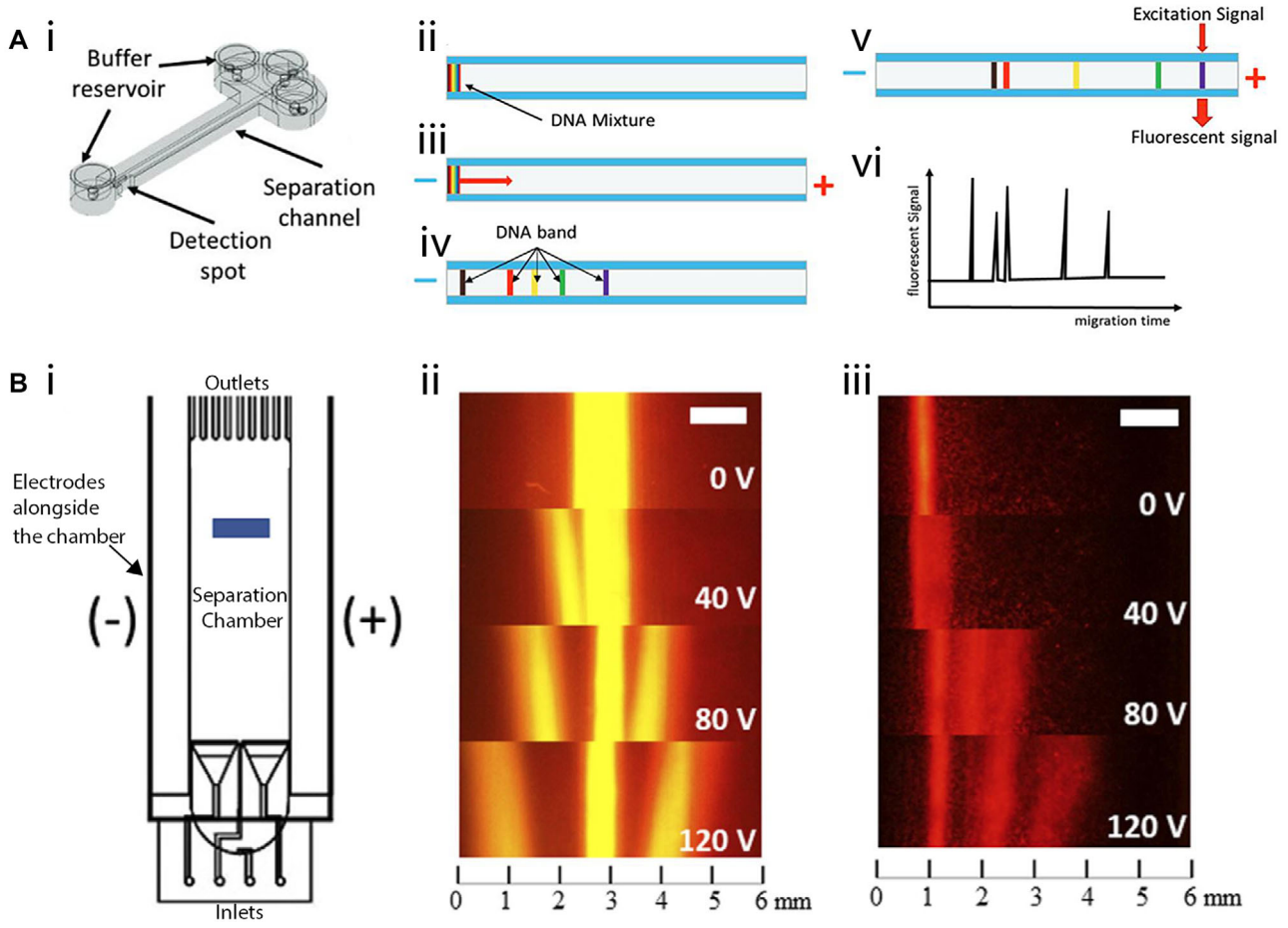

FIGURE 6 3D-printed electrophoretic devices. (A-i) Schematic of the 3D-printed device for gel electrophoretic separation of DNA. (ii-iv) Fluorescently-labeled DNA fragments introduced into the separation channel are driven through the channel by applying voltage and separated. (v-vi) Fluorescence is used to detect the fragments. Reproduced with permission from [75]. Copyright 2016, the authors. Published under Attribution-NonCommercial-NoDerivatives 4.0 International license (CC BY-NC-ND 4.0) (B-i) Schematic of the 3D-printed free-flow electrophoretic system used to (ii) separate fluorescence dyes and (iii) fluorescently-labeled amino acids. Adapted with permission from [76]. Copyright 2020, the authors. Published under Creative Commons Attribution 4.0 International license (CC BY 4.0)

material using the MultiJet printing technology [76]. This free-flow electrophoresis system consists of inlets for buffer and sample, a separation chamber, and outlets that guide the separate fractions into designated collection wells (see Figure 6B-i). Alongside the device, two platin wires (functioning as electrodes) are installed and separated from the separation chamber using a polycarbonate membrane. The principle of this free-flow electrophoresis technique is straightforward: Applying a voltage creates a positive pole on one side of the separation chamber and a negative pole on the other side, allowing researchers to separate differently charged molecules. In this proof-of-concept study, the fluorescence dyes rhodamine B, pyronine Y, and sulforhodamine B (Figure 6B-ii), and the fluorescently-labeled amino acids arginine, glycine, and glutamate (Figure 6B-iii) could be successfully segregated.

4.2 | Biosensors and point-of-care diagnostics

Various biosensor systems designed to detect diverse target molecules such as DNA [79], proteins [80], carbohydrates [81, 82], and bacteria [26] have also been successfully integrated into 3D- printed systems. The integration of optical and electrochemical biosensors into microfluidic and miniaturized 3D-printed systems has been an area of increasing interest in recent years [83]. An example of such an optical biosensor was presented by Arshavsky-Graham et al. who deployed a photonic porous silicon (PSi) chip as the transducing element and integrated the chip into a 3D-printed system (see Figure 7A-i) [80]. These PSi-chips consist of a porous nanostructure that is preferential for capture probe (e.g. aptamers, antibodies) immobilization due to its high surface area [84]. Molecule binding (Fig-

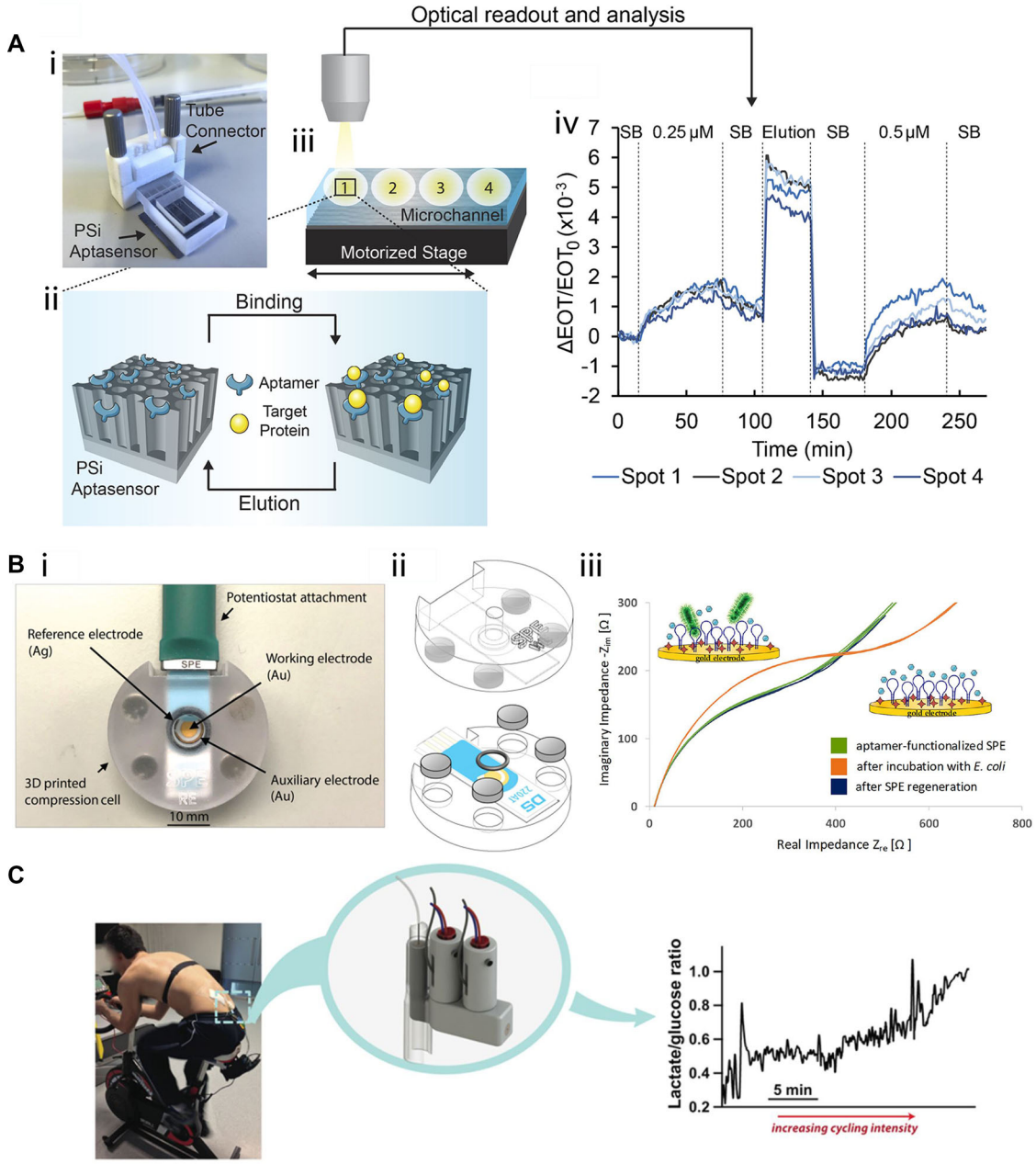

FIGURE 7 3D printing for biosensing applications. (A-i) Photograph of the 3D-printed device with integrated photonic PSi-chips. (A-ii) The chip's silicon nanostructure is functionalized with aptamers specific for target proteins exhibiting a histidine-tag. (A-iii) Measurements are conducted at different spots along the microfluidic channel, and optical readout and analysis are performed to (A-iv) monitor target molecule binding by tracking changes in the refractive index within the porous layer. Reproduced with permission from [80]. Copyright 2021, the authors. Published under Creative Commons Attribution 4.0 International license (CC BY 4.0). (B-i) Photograph of the impedance-based biosensor for *E. coli* detection in which (B-ii) the SPE is placed between two 3D-printed parts. The system is held together by disc magnets and sealed by using an o-ring. (B-ii) Presence of *E. coli* cells onto the aptamer-decorated SPE gold surface is detected by monitoring changes in the impedance signal. Adapted with permission from [26]. Copyright 2020, the authors. Published under Creative Commons Attribution 4.0 International license (CC BY 4.0). (C) Microdialysis probes and lactate and glucose biosensors are integrated into a 3D-printed system to analyze lactate and glucose levels in subcutaneous tissue during a cycling exercise. Reproduced with permission from [85]. Copyright 2015, American Chemical Society. Published under Creative Commons Attribution 4.0 International license (CC BY 4.0)

ure 7A-ii) to these capture probes can be monitored in a label-free manner by illuminating the chips (Figure 7A-iii) and recording unique reflectance spectra using a spectrometer. The reflectance spectra are then analyzed to monitor refractive index changes within the porous nanostructure caused by target molecules binding to the respective capture probe (see Figure 7A-iv). In the presented work, the PSi-chip was integrated by bonding the 3D-printed device (created by MultiJet printing) with microfluidic channels open to their bottom onto the chip's surface using an optical adhesive. Subsequently, the nanostructured silicon surface was functionalized using an established aptamer binding to histidine-tags in proteins. Optical readout and analysis were also enabled by the translucent properties of the 3D-printed material. Both the selectivity and sensitivity of this 3D-printed microfluidic biosensing system were superior to the previously used system; moreover, biosensor regeneration was also demonstrated using an imidazole-containing buffer to elute the target molecule from the sensor surface. In general, this same concept can be applied for various target molecules simply by employing designated aptamers or other capture probes.

In another work, Siller et al. similarly demonstrated how an electrochemical impedance spectroscopy (EIS) biosensor for bacteria detection could be integrated into a 3D-printed system using the same printing technology [26]. Figure 7B-i and -ii both illustrate the 3D-printed device, which consisted of a screen-printed electrode (SPE) placed between two 3D-printed parts held together by magnets. The upper part contained a cavity, allowing the addition of defined volumes of buffer or bacteria suspension onto the electrode. The gold surface of the SPE was functionalized with aptamers specific for *Escherichia coli* to facilitate the detection of this bacterial species by EIS measurements (Figure 7B-iii) at cell densities between 10^5 and 10^8 cells mL^{-1}. In contrast, a different bacterium, *Enterococcus faecalis*, remained indetectable even at high concentrations (10^8 cells mL^{-1}), demonstrating the system's selectivity. This project also highlights one of the particular strengths of this approach: design flexibility. The static system (described above) was adjusted to create a flow cell by integrating inlets and outlets, enabling automated control of the fluid flow and introducing defined volumes (e.g. washing buffer and sample suspensions) by connecting the flow cell to pumps. For instance, this system could be used to adjust concentrations automatically, run concentration gradients, or switch between dynamic (flow) and static (without flow) states. Moreover, a micromixer was also integrated, enabling homogenous mixing of fluids before being introduced onto the SPE surface.

3D printing has even been applied to fabricate systems that can potentially be used as wearable biosensors. For example, Gowers et al. have reported their successful integration of microdialysis probes, as well as glucose and lactate biosensors, into a 3D-printed system [85]. Their device was attached directly to the human body, and facilitated the measurement of lactate and glucose levels in the subcutaneous tissue during cycling exercises, as shown in Figure 7C. Tracking both of these biomarkers is of particular interest for sports- and fitness-related monitoring, since lactate is produced during intense exercise when there is not sufficient oxygen in the tissues and aerobic metabolism cannot provide enough energy for the body [85]. The described biosensor system demonstrates a concrete step towards point-of-care applications which would potentially permit individual physicians to perform monitoring and diagnostics on individual patients without relying on centralized laboratories. Indeed, 3D printing has already been used for various applications in this realm—including blood plasma separation, concentration and detection of bacteria from blood, or diagnosis of drug-resistant bacteria [86], underscoring yet again the tremendous versatility of this technology.

5 | CONCLUDING REMARKS

In this review, we have sought to offer some insights into promising recent developments of 3D printing technology for the fabrication of miniaturized and microfluidic tools in the biotechnology field. Various devices for different applications—ranging from cell culture to biosensors and diagnostics—have already been realized in labs across the world, thanks to the ever-increasing variety of available materials and printing technologies. Compared to soft lithography using PDMS, 3D printing allows for the relatively automated and straightforward fabrication of devices, within a single step and without the requirement for a master mold or cleanroom procedures.

Having said that, some technological barriers do continue to limit the widespread adoption of 3D printing for microfluidic systems—and, to date, no 3D printing technology and material have managed to successfully package and duplicate all the beneficial properties realized through PDMS (e.g. very high resolution, biocompatibility, gas permeability, optical clarity, and flexibility) [13]. Nevertheless, the authors firmly believe that the principle obstructions which currently impede widespread adoption of this technology can, and will, be substantially overcome within the next few years. Only the future will reveal if 3D printing remains a technique primarily used for experiment-specific rapid prototyping, or if 3D printing will finally enable rapid manufacturing of customized 3D-printed tools for market-wide applications such as cell culture, biosensors, or point-of-care diagnostics—but

there is unquestionably room for great optimism about the promise of this young and rapidly advancing technology.

ACKNOWLEDGMENTS

The authors acknowledge the financial support through the Emmy Noether Programme (346772917).

Open access funding enabled and organized by Projekt DEAL.

CONFLICT OF INTEREST

The authors declare no conflict of interest.

DATA AVAILIBILTY STATEMENT

Data sharing not applicable – no new data generated.

ORCID

Christopher Heuer https://orcid.org/0000-0002-3694-0008

REFERENCES

1. Hull, C. W. Apparatus for Production of Three-Dimensional Objects by Stereolithography. US Patent US4575330A; 1984.
2. Hull, C. On stereolithography. Virtual Phys. Prototyp. 2012, 7, 177.
3. Hull, C. W. The birth of 3D printing. Res. Technol. Manag. 2015, 58, 25–29.
4. Crump, S. S. Apparatus and Method for Creating Three-Dimensional Objects. US Patent US5121329A; 1989.
5. Deckard, C. R. Apparatus for Producing Parts by Selective Sintering. US Patent US5597589A; 1986.
6. Sachs, E. M., Haggerty, J. S., Cima, M. J., Williams, P. A. T*hree-Dimensional Printing Techniques*. US Patent US5204055A; 1989.
7. Gong, H., Bickham, B. P., Woolley, A. T. and Nordin, G. P., Custom 3D printer and resin for 18 μm x 20 μm microfluidic flow channels. Lab Chip 2017, 17, 2899–2909.
8. Bhanvadia, A. A., Farley, R. T., Noh, Y. and Nishida, T., High-resolution stereolithography using a static liquid constrained interface. Commun. Mater. 2021, 2, 1–7.
9. Takagishi, K. and Umezu, S., Development of the improving process for the 3D printed structure. Sci. Rep. 2017, 7, 1–10.
10. Mazzanti, V., Malagutti, L. and Mollica, F., FDM 3D printing of polymers containing natural fillers: a review of their mechanical properties. Polymers. 2019, 11, 1094.
11. Šafka, J., Ackermann, M., Bobek, J., Seidl, M., et al. Use of composite materials for FDM 3D print technology. Mater. Sci. Forum 2016, 862, 174–181.
12. Chen, M. Y., Skewes, J., Daley, R., Woodruff, M. A., et al. Three-dimensional printing versus conventional machining in the creation of a meatal urethral dilator: development and mechanical testing. Biomed. Eng. Online 2020, 19, 1–11.
13. Bhattacharjee, N., Urrios, A., Kang, S. and Folch, A., The upcoming 3D-printing revolution in microfluidics. Lab Chip 2016, 16, 1720–1742.
14. Beauchamp, M. J., Nordin, G. P. and Woolley, A. T., Moving from millifluidic to truly microfluidic sub-100-μm cross-section 3D printed devices. Anal. Bioanal. Chem. 2017, 409, 4311–4319.
15. Siller, I. G., Enders, A., Steinwedel, T., Epping, N. - M., et al. Real-time live-cell imaging technology enables high-throughput screening to verify in vitro biocompatibility of 3D printed materials. Materials. 2019, 12, 2125.
16. Gross, B. C., Erkal, J. L., Lockwood, S. Y., Chen, C., et al. Evaluation of 3D printing and its potential impact on biotechnology and the chemical sciences. Anal. Chem. 2014, 86, 3240–3253.
17. Krujatz, F., Lode, A., Seidel, J., Bley, T., et al. Additive Biotech—Chances, challenges, and recent applications of additive manufacturing technologies in biotechnology. N. Biotechnol. 2017, 39, 222–231.
18. Romanov, V., Samuel, R., Chaharlang, M., Jafek, A. R., et al. FDM 3D printing of high-pressure, heat-resistant, transparent microfluidic devices. Anal. Chem. 2018, 90, 10450–10456.
19. He, Y., Wu, Y., Fu, J. Z., Gao, Q., et al. Developments of 3D printing microfluidics and applications in chemistry and biology: a review. Electroanalysis 2016, 28, 1658–1678.
20. Au, A. K., Huynh, W., Horowitz, L. F. and Folch, A., 3D-printed microfluidics. Angew. Chem. Int. Ed. 2016, 55, 3862–3881.
21. Kuo, A. P., Bhattacharjee, N., Lee, Y. S., Castro, K., et al. High-precision stereolithography of biomicrofluidic devices. Adv. Mater. Technol. 2019, 4, 11.
22. Mehta, V. and Rath, S. N. 3D printed microfluidic devices: a review focused on four fundamental manufacturing approaches and implications on the field of healthcare. Bio-Design Manuf. 2021, 4, 311–343.
23. Urrios, A., Parra-Cabrera, C., Bhattacharjee, N., Gonzalez-Suarez, A. M., et al. 3D-printing of transparent bio-microfluidic devices in PEG-DA. Lab Chip 2016, 16, 2287–2294.
24. Samper, I. C., Gowers, S. A. N., Rogers, M. L., Murray, D. R. K., et al. 3D printed microfluidic device for online detection of neurochemical changes with high temporal resolution in human brain microdialysate. Lab Chip 2019, 19, 2038–2048.
25. Enders, A., Siller, I. G., Urmann, K., Hoffmann, M. R., et al. 3D printed microfluidic mixers-a comparative study on mixing unit performances. Small 2019, 15, 9.
26. Siller, I. G., Preuss, J. A., Urmann, K., Hoffmann, M. R., et al. 3D-printed flow cells for aptamer-based impedimetric detection of E. coli Crooks Strain. Sensors 2020, 20, 16.
27. Stratasys, Our materials. https://www.stratasys.com/materials/search, accessed June 2021.
28. 3D Systems Inc. What are the Benefits of MultiJet Printing?. 3D Systems Inc.; https://www.3dsystems.com/resources/information-guides/multi-jet-printing/mjp?smtNoRedir=1&_ga=2.164098874.461882064.1624609672-2059785067.1603350887, accessed June 2021.
29. Ukita, Y., Takamura, Y. and Utsumi, Y., Direct digital manufacturing of autonomous centrifugal microfluidic device. Jpn. J. Appl. Phys. 2016, 55, 6.
30. Sochol, R. D., Sweet, E., Glick, C. C., Venkatesh, S., et al. 3D printed microfluidic circuitry via multijet-based additive manufacturing. Lab Chip 2016, 16, 668–678.
31. Walczak, R. and Adamski, K., Inkjet 3D printing of microfluidic structures-on the selection of the printer towards printing your own microfluidic chips. J. Micromech. Microeng. 2015, 25, 11.
32. Yin, P. J., Zhao, L., Chen, Z. Z., Jiao, Z. Q., et al. Simulation and practice of particle inertial focusing in 3D-printed serpentine microfluidic chips via commercial 3D-printers. Soft Matter 2020, 16, 3096–3105.

33. Anciaux, S. K., Geiger, M. and Bowser, M. T., 3D printed micro free-flow electrophoresis device. Anal. Chem. 2016, 88, 7675–7682.
34. Bressan, L. P., Adamo, C. B., Quero, R. F., de Jesus, D. P., et al. A simple procedure to produce FDM-based 3D-printed microfluidic devices with an integrated PMMA optical window. Anal. Methods 2019, 11, 1014–1020.
35. Zeraatkar, M., Filippini, D. and Percoco, G., On the impact of the fabrication method on the performance of 3D printed mixers. Micromachines 2019, 10, 10.
36. Nelson, M. D., Ramkumar, N. and Gale, B. K., Flexible, transparent, sub-100 μm microfluidic channels with fused deposition modeling 3D-printed thermoplastic polyurethane. J. Micromech. Microeng. 2019, 29, 8.
37. Li, F., Smejkal, P., Macdonald, N. P., Guijt, R. M., et al. One-step fabrication of a microfluidic device with an integrated membrane and embedded reagents by multimaterial 3D printing. Anal. Chem. 2017, 89, 4701–4707.
38. Ruiz, C., Kadimisetty, K., Yin, K., Mauk, M. G., et al. Fabrication of hard-soft microfluidic devices using hybrid 3D printing. Micromachines 2020, 11, 11.
39. Salentijn, G. I. J., Oomen, P. E., Grajewski, M. and Verpoorte, E., Fused deposition modeling 3d printing for (bio)analytical device fabrication: procedures, materials, and applications. Anal. Chem. 2017, 89, 7053–7061.
40. Macdonald, N. P., Cabot, J. M., Smejkal, P., Guijt, R. M., et al. Comparing microfluidic performance of three-dimensional (3D) printing platforms. Anal. Chem. 2017, 89, 3858–3866.
41. Kotz, F., Mader, M., Dellen, N., Risch, P., et al. Fused deposition modeling of microfluidic chips in polymethylmethacrylate. Micromachines 2020, 11, 12.
42. Quero, R. F., da Silveira, G. D., da Silva, J. A. F., da Jesus, D. P. Understanding and improving FDM 3D printing to fabricate high-resolution and optically transparent microfluidic devices. Lab Chip 2021.21:3715–3729.
43. Piironen, K., Haapala, M., Talman, V., Järvinen, P., et al. Lab on a chip cell adhesion and proliferation on common 3D printing materials used in stereolithography of microfluidic devices. Lab Chip 2020, 20, 2372–2382.
44. Rimington, R. P., Capel, A. J., Player, D. J., Bibb, R. J., et al. Feasibility and biocompatibility of 3D-printed photopolymerized and laser sintered polymers for neuronal, myogenic, and hepatic cell types. Macromol. Biosci. 2018, 18, 1800113.
45. Gul, J. Z., Sajid, M., Rehman, M. M., Siddiqui, G. U., et al. 3D printing for soft robotics - a review. Sci. Technol. Adv. Mater. 2018, 19, 243–262.
46. Gulyas, M., Csiszer, M., Mehes, E. and Czirok, A., Software tools for cell culture-related 3D printed structures. PLoS One 2018, 13, e0203203.
47. Siller, I. G., Enders, A., Gellermann, P., Winkler, S., et al. Characterization of a customized 3D-printed cell culture system using clear, translucent acrylate that enables optical online monitoring. Biomed. Mater. 2020, 15, 55007.
48. Panjan, P., Virtanen, V. and Sesay, A. M., Towards microbioprocess control: an inexpensive 3D printed microbioreactor with integrated online real-Time glucose monitoring. Analyst 2018, 143, 3926–3933.
49. Frey, L. J., Vorländer, D., Ostsieker, H., Rasch, D., et al. 3D-printed micro bubble column reactor with integrated microsensors for biotechnological applications: from design to evaluation. Sci. Rep. 2021, 11, 7276.
50. Kuhlmann, W., Meyer, H. D., Bellgardt, K. H. and Schügerl, K., On-line analysis of yeast growth and alcohol production. J. Biotechnol. 1984, 1, 171–185.
51. Qian, X., Nguyen, H. N., Song, M. M., Hadiono, C., et al. Brain-region-specific organoids using mini-bioreactors for modeling ZIKV exposure. Cell 2016, 165, 1238–1254.
52. Drost, J. and Clevers, H., Organoids in cancer research. Nat. Rev. Cancer 2018, 18, 407–418.
53. Wang, Y. I., Abaci, H. E. and Shuler, M. L., Microfluidic blood-brain barrier model provides in vivo-like barrier properties for drug permeability screening. Biotechnol. Bioeng. 2017, 114, 184–194.
54. Gensler, M., Leikeim, A., Möllmann, M., Komma, M., et al. 3D printing of bioreactors in tissue engineering: a generalised approach. PLoS One 2020, 15, e0242615.
55. Siller, I. G., Epping, N. M., Lavrentieva, A., Scheper, T., et al. Customizable 3D-printed (Co)cultivation systems for in vitro study of angiogenesis. Materials. 2020, 13, 1–17.
56. Alessandri, K., Feyeux, M., Gurchenkov, B., Delgado, C., et al. A 3D printed microfluidic device for production of functionalized hydrogel microcapsules for culture and differentiation of human Neuronal Stem Cells (hNSC). Lab Chip 2016, 16, 1593–1604.
57. Lavrentieva, A., Fleischhammer, T., Enders, A., Pirmahboub, H., et al. Fabrication of stiffness gradients of GelMA hydrogels using a 3D printed micromixer. Macromol. Biosci. 2020, 20, 2000107.
58. Razavi Bazaz, S., Rouhi, O., Raoufi, M. A., Ejeian, F., et al. 3D printing of inertial microfluidic devices. Sci. Rep. 2020, 10, 14.
59. Aranda Hernandez, J., Heuer, C., Bahnemann, J., Szita, N. Microfluidic Devices as Process Development Tools for Cellular Therapy Manufacturing. In: Advances in Biochemical Engineering/Biotechnology; 2021.
60. Chiu, P. L., Chang, C. H., Lin, Y. L., Tsou, P. H., et al. Rapid and safe isolation of human peripheral blood B and T lymphocytes through spiral microfluidic channels. Sci. Rep. 2019, 9, 1–10.
61. Nathamgari, S. S. P., Dong, B., Zhou, F., Kang, W., et al. Isolating single cells in a neurosphere assay using inertial microfluidics. Lab Chip 2015, 15, 4591–4597.
62. Yin, L., Au, W. Y., Yu, C. C., Kwon, T., et al. Miniature auto-perfusion bioreactor system with spiral microfluidic cell retention device. Biotechnol. Bioeng. 2021, 118, 1951–1961.
63. Lee, W., Kwon, D., Choi, W., Jung, G. Y., et al. 3D-Printed micro fluidic device for the detection of pathogenic bacteria using size-based separation in helical channel with trapezoid cross-section. Sci. Rep. 2015, 5, 1–7.
64. Enders, A., Preuss, J. - A., Bahnemann, J., 3D printed microfluidic spiral separation device for continuous, pulsation-free and controllable CHO cell retention. Micromachines 2021, 12, 1060.
65. Tamay, D. G., Dursun Usal, T., Alagoz, A. S., Yucel, D., et al. 3D and 4D printing of polymers for tissue engineering applications. Front. Bioeng. Biotechnol. 2019, 0, 164.
66. Zaszczyńska, A., Moczulska-Heljak, M., Gradys, A., Sajkiewicz, P., Advances in 3d printing for tissue engineering. Materials 2021, 14, 3149.
67. Salmean, C. and Dimartino, S., 3D-printed stationary phases with ordered morphology: state of the art and future development in liquid chromatography. Chromatographia 2019, 82, 443–463.

68. Kalsoom, U., Nesterenko, P. N. and Paull, B., Current and future impact of 3D printing on the separation sciences. Trends Anal. Chem. 2018, 105, 492–502.
69. Lucklum, F., Janssen, S., Lang, W. and Vellekoop, M. J., Miniature 3D gas chromatography columns with integrated fluidic connectors using high-resolution stereolithography fabrication. Procedia Eng., 2015, 120, 703–706.
70. Schure, M. R., Maier, R. S., How does column packing microstructure affect column efficiency in liquid chromatography? J. Chromatogr. A 2006, 1126, 58–69.
71. Simon, U. and Dimartino, S., Direct 3D printing of monolithic ion exchange adsorbers. J. Chromatogr. A 2019, 1587, 119–128.
72. Simon, U., Scorza, L. C. T., Teworte, S., McCormick, A. J., et al. Demonstration of protein capture and separation using three-dimensional printed anion exchange monoliths fabricated in one-step. J. Sep. Sci. 2021, 44, 1078–1088.
73. Nawada, S., Dimartino, S. and Fee, C., Dispersion behavior of 3D-printed columns with homogeneous microstructures comprising differing element shapes. Chem. Eng. Sci. 2017, 164, 90–98.
74. Wang, H., Cocovi-Solberg, D. J., Hu, B. and Miró, M., 3D-printed microflow injection analysis platform for online magnetic nanoparticle sorptive extraction of antimicrobials in biological specimens as a front end to liquid chromatographic assays. Anal. Chem. 2017, 89, 12541–12549.
75. Adamski, K., Kubicki, W. and Walczak, R., 3D printed electrophoretic lab-on-chip for DNA separation. Procedia Eng. 2016, 168, 1454–1457.
76. Preuss, J., Nguyen, G. N., Berk, V. and Bahnemann, J., Miniaturized free-flow electrophoresis: production, optimization, and application using 3D printing technology. Electrophoresis 2021, 42, 305–314.
77. Barbaresco, F., Cocuzza, M., Pirri, C. F. and Marasso, S. L., Application of a micro free-flow electrophoresis 3d printed lab-on-a-chip for micro-nanoparticles analysis. Nanomaterials 2020, 10, 1277.
78. Islinger, M., Eckerskorn, C. and Völkl, A., Free-flow electrophoresis in the proteomic era: a technique in flux. Electrophoresis 2010, 31, 1754–1763.
79. Loo, A. H., Chua, C. K., Pumera, M., DNA biosensing with 3D printing technology. Analyst 2017, 142, 279–283.
80. Arshavsky-Graham, S., Enders, A., Ackerman, S., Bahnemann, J., et al. 3D-printed microfluidics integrated with optical nanostructured porous aptasensors for protein detection. Microchim. Acta 2021, 188, 1–12.
81. Nesaei, S., Song, Y., Wang, Y., Ruan, X., et al. Micro additive manufacturing of glucose biosensors: a feasibility study. Anal. Chim. Acta 2018, 1043, 142–149.
82. Cardoso, R. M., Silva, P. R. L., Lima, A. P., Rocha, D. P., et al. 3D-Printed graphene/polylactic acid electrode for bioanalysis: biosensing of glucose and simultaneous determination of uric acid and nitrite in biological fluids. Sens. Actuators, B Chem. 2020, 307, 127621.
83. Muñoz, J., Pumera, M., 3D-printed biosensors for electrochemical and optical applications. TrAC - Trends Anal. Chem. 2020, 128, 115933.
84. Arshavsky-Graham, S., Massad-Ivanir, N., Segal, E., Weiss, S., Porous silicon-based photonic biosensors: current status and emerging applications. Anal. Chem. 2019, 91, 441–467.
85. Gowers, S. A. N., Curto, V. F., Seneci, C. A., Wang, C., et al. 3D printed microfluidic device with integrated biosensors for online analysis of subcutaneous human microdialysate. Anal. Chem. 2015, 87, 7763–7770.
86. Chan, H. N., Tan, M. J. A., Wu, H. Point-of-care testing: applications of 3D printing. Lab Chip 2017, 17, 2713–2739.
87. Hällgren S., Pejryd L., Ekengren J. 3D Data Export for Additive Manufacturing - Improving Geometric Accuracy. Procedia CIRP. 2016;50:518–523.

How to cite this article: Heuer, C., Preuß, J-A., Habib, T., Enders, A., Bahnemann, J. 3D printing in biotechnology—An insight into miniaturized and microfluidic systems for applications from cell culture to bioanalytics. Eng Life Sci. 2021;1–16. https://doi.org/10.1002/elsc.202100081